Classifying HCM Subtypes via Left Ventricular Two-Dimensional Curvature and Dynamic Time Wrapping

Min Wan, Yuli Yang, Xiaodan Zhao, Shuang Leng, Jun-Mei Zhang, Ru San Tan, Liang Zhong

Abstract

Identification of Hypertrophic cardiomyopathy (HCM) morphological subtypes has the same significance as diagnosis HCM due to the close relation of subtypes and genetic mutations. This study aims to automatically classify HCM cases into subtypes via two-dimensional endocardial curvature and dynamic time wrapping (DTW). A total of 19 HCM patients underwent cardiac magnetic resonance (CMR) scans. Endocardial boundaries were delineated on long axis images. Endocardial curvatures were computed. Dynamic time wrapping and its variant soft-DTW were used to quantify the dissimilarity between a pair of endocardial curvature series. The dissimilarity was utlized in classifiers. The classifier using DTW has a 0.84 in-sample accuracy and 0.58 out-of-sample accuracy. Soft-DTW has a 0.79 in-sample accuracy and 0.68 out-of-sample accuracy. We envision the use of this method in current clinical practice to improve the subtype identification efficiency and effectiveness.

1. Introduction

Being a primary disease of the cardiac sarcomere[1, 2], Hypertrophic cardiomyopathy (HCM) affects approximately one individual out of 500. The annual mortality rate is approximately 1-2%[3]. HCM is often characterized by the thickening and enlarged left ventricular (LV) myocardium [1, 3–5]. Asymptomatic HCM may progress to fibrosis and impairment of cardiac function, resulting in sudden cardiac death. Impaired LV cardiac function and left ventricular outflow tract (LVOT) obstruction are possible clinical symptoms of HCM. But assessment and diagnosis of HCM is typically performed by measuring LV wall thickness in echocardiagraphy.The pattern of ventricular hypertrophy is highly variable and broadly categorized into the morphological subtypes: reverse curvature, sigmoid, and neutral [6].

Identification of the morphological subtype may have same significance of the diagnosis itself. Since morphological subtypes are related to genetic mutation. [6] showed that the majority (79%) of reverse curvature subtype were found to harbor a certain genetic mutation. While relatively a small percentage (16%) of other subtypes have such mutation. The frequency of various genetic mutations in all subtypes was reported in [6]. That meaningful results suggest subsequent genetic counseling and genetic testing after diagnosis of HCM. Manual identification of morphological subtypes could be performed via examining echocardiography.

Echocardiagraphy has limitations in diagnosing HCM as well as identifying morphological subtypes. Due to the difficulty to visualize the hypertrophied myocardium part, echocardiography probably underestimate the extent of the LV wall thickening, especially for patients with the hypertrophied anterolateral wall [7]. Due to its high spatial resolution, intrisic blood-to-tissue contrast and high reproducibility, cardiac magneticc resonance (CMR) has been considered the non-invasive gold standard for evaluating cardiac volume and ejection fraction, and deformation using feature tracking technique [8–11]. All above advantages make CMR a preferred imaging modality in identifying morphological subtypes [12]. Furthermore, three-dimensional geometric characteristics could be assessed more accurately, both regionally and globally [12–16]. In our previous studies [17, 18], we also report the regional wall thickness as a sensitive marker for diagnosis HCM and identification of subtypes.

However, all above indicators strongly depend on the establishment of the myocardium model, which demands delineation of both endocardium and epicardium. However, to delineate epicardium is not a trivial task. The boundary of epicardium is not obvious as that of endocardium. Manual delineation of epicardium requires experienced experts. Automatic epicardium delineation is still under experimental stage. Meanwhile, endocardium is easier to identify due to the high contrast between myocardium and blood pool. A lot of studies constribute to automatic endocardium segmentation. The demand to classify HCM subtypes using only endocardial characteristics motivates our study.

In this study, we proposed a method to classify HCM subtypes using only two-dimensional endocardial curves. Endocardial curves were delineated on three-chamber long axis images. Curvature on the endocardial curves were computed. The dissimilarity among curvature series of all cases was evaluated and utilized in subsequent classifiers. The remainder of this paper is organized as follows. Section 2 describes the methodology including (a) image

 ISSN: 2325-887X DOI: 10.22489/CinC.2019.188

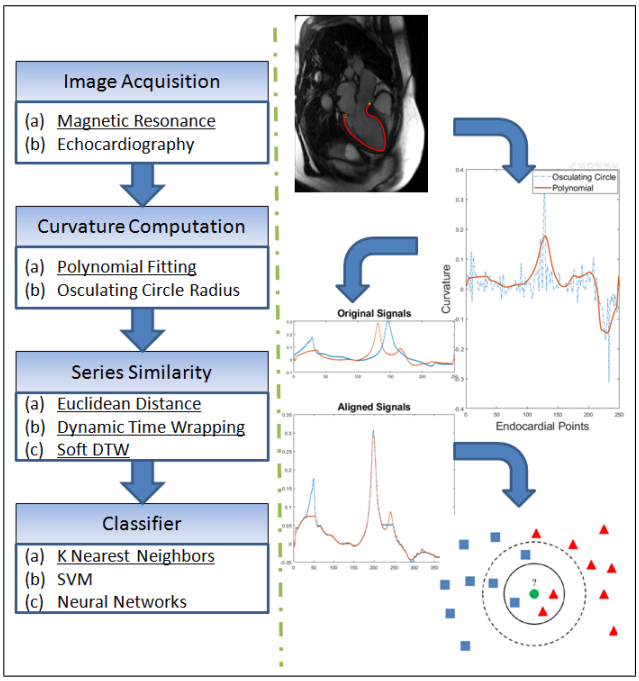

Figure 1. Flowchart of the proposed method. Several alternative implementations are provided for each stage. The implementations we ultilized are underlined.

acquisition and processing; (b) curvature computation; (c) quantifying dissimilarity/discrepancy between two curvature series; (d) classifying HCM subtypes automatically. Section 3 provides the experimental results and both qualitative and quantitative validation. The performance of algorithm is evaluated. Section 4 concludes this article.

2. Methods

The method proposed in this study consists of four stages: (1) Image acquisition and processing; (2) Curvature computation; (3) Quantifying similarity between curvature series; (4) Classifying subtypes based on similarity. The flowchart describing our method is shown in Figure 1. Alternative implementations are also included with illustration. Each stage will now be described in detail.

2.1. Study Population

The SingHealth Centralized Institutional Review Board approved this study for human research. All 19 patients were provided with comprehensive information about the study as well as the data collection and usage. The MR data are deposited in hospital and are available for research and educational purposes. Patients mean age was 51 $\pm$ 13 years, and 7 were male. All 19 cases were categorized by our senior HCM consultant as sigmoid (n = 6), reverse curvature (n = 8) or neutral (n = 5), according to the HCM

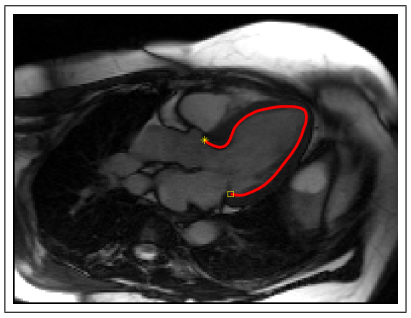

Figure 2. Long axis left ventricular endocardial boundary starting at mitral posterior (square marker), ending at aortic anterior (asterisk marker)

subtype description in [6].

2.2. MR Scan and Processing

Cardiovascular magnetic resonance was performed in all patients on a 1.5T scanner (Avanto, Germany) using steady state, free precession (SSFP) cine gradient echo sequences. Parallel short axis images as well as radial long axis images(two-chamber,three-chamber,four-chamber) were acquired. Only three-chamber long axis image was used for analysis. The minimal requirement suggests that methods in this study could be adapted for echocardiography without much effort.

Left ventricular endocardial boundary were delineated by trained experts using CMRtools (Cardiovascular Solution, UK). The boundary curve was open at the atrioventricular annulus. Experts delineated the endocardial curve from posterior of mitral valvar orifice to anterior of aortic valvar orifice. An example of the delineated endocardial curve was shown in Figure 2. The middle of the curve was at left ventricular apex and the latter half of the curve was interventricular septum part. This guideline guaranteed the same direction for endocardial curves in all cases. Since the curve was in a counterclockwise direction, the obtained curvature shall be positive mostly.

2.3. Curvature Computation

Two-dimensional curvature of a planar curve could measure how sensitive or fast the tangent vector of the curve is rotating. The descriptive terms ”convex” and ”concave” frequently used in HCM myocardial morphology could be quantitized using curvature. Since the endocardial curves obtained were discrete curves consisting of discrete points, no analytic/parametric representation was available. The curvature could only be estimated using other points in some neighborhood instead of computed as in differential geometry. Discrete curvature estimation methods can be based on (1) derivative of the tangent angle; (2) radius of

the osculating circle; (3) derivative of the curve. We chose the derivative of the curve implementation. For all 19 patients, we computed the endocardial curvature.

2.4. Quantifying Dissimilarity between Series

We can observe inter-subtype dissimilarity qualitatively. To quantify the dissimilarity, we utilize dynamic time wrapping (DTW) algorithm [19, 20]. Given two series $\mathbf{x} = (\mathbf{x_1}, \ldots, \mathbf{x_n}) \in \mathbf{R^n}$ and $\mathbf{y} = (\mathbf{y_1}, \ldots, \mathbf{y_m}) \in \mathbf{R^m}$, the cost matrix is defined as

$$\Delta(\mathbf{x}, \mathbf{y}) := [\delta(\mathbf{x_i}, \mathbf{y_j})]_{\mathbf{ij}} \in \mathbf{R^{n \times m}} \tag{1}$$

The inner product $\langle A, \Delta(\mathrm{x}, \mathrm{y}) \rangle$ provides a score for the alignment matrix A. DTW is the least score among all possible alignment matrices. Another alignment algorithm Global Alignment kernel (GAK) [21] takes into account of all alignment matrices.

$$\begin{aligned} \mathrm{DTW}(\mathrm{x}, \mathrm{y}) &:= \min_{A \in A_{n,m}} \langle A, \Delta(\mathrm{x}, \mathrm{y}) \rangle \\ k^{\gamma}_{\mathrm{GA}}(\mathrm{x}, \mathrm{y}) &:= \sum_{A \in A_{n,m}} e^{-\langle A, \Delta(\mathrm{x}, \mathrm{y}) \rangle / \gamma} \end{aligned} \tag{2}$$

Soft DTW [22] unifies the above two alignment and provides a smoothed dissimilarity measure.

$$\min{}^{\gamma} \{a_1, \ldots, a_n\} := \begin{cases} \min_{i \le n} a_i, & \gamma = 0 \\ -\gamma \log \sum_{i=1}^{n} e^{-a_i/\gamma}, & \gamma > 0 \end{cases} \tag{3}$$

γ-soft-DTW is defined as

$$\mathrm{dtw}_{\gamma}(\mathrm{x}, \mathrm{y}) := \min{}^{\gamma} \{\langle \mathrm{A}, \Delta(\mathrm{x}, \mathrm{y}) \rangle, \mathrm{A} \in \mathrm{A}_{\mathrm{n,m}}\} \tag{4}$$

Two curvature series from two HCM cases were shown in Figure 3 as well as their DTW alignment. The dissimilarity was used to classify the curvature series.

3. Results

Cine MR images were acquired for all 19 HCM patients and only three-chamber long axis ED frame was processed. The average of manual delineation time using CMRTools is about half minute. Curvature computation average time is 5 ms on a 2.5 GHz CPU desktop. The average time of DTW for one case is 0.7ms. Soft DTW took about 0.15s for one case. Compared to the three-dimensional geometric descriptors and shape reconstruction, two-dimensional curvature based methods are largely efficient.

We used three types of dissimilarity measures in this study, (1) Euclidean distance without alignment; (2) DTW distance; (3) soft DTW distance.

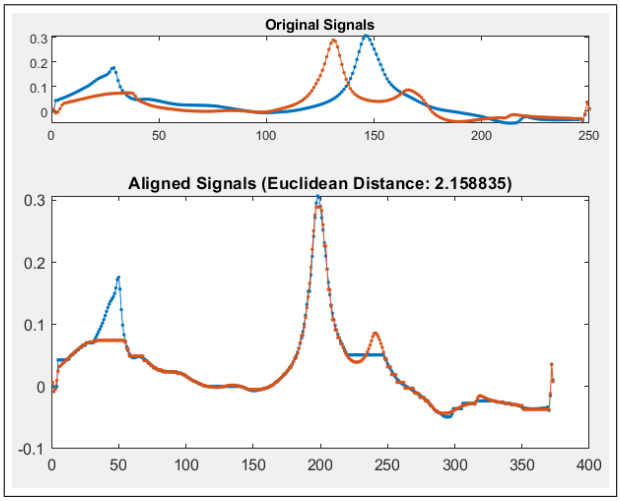

Figure 3. Two curvature series and their DTW alignment

All 19 cases were sub-categorized by a senior HCM consultant. Classic K-nearest neighbors algorithm was also trained to classifiy 19 cases into 3 subtypes. Classifier performances were evaluated by both in-sample accuracy and out-of-sample accuracy. Out-of-sample experiments were conducted using leave-one-out (LOO) cross-validation. The classifier accuracy for all three dissimilarity measures were listed in Table 1. Euclidean distance without alignment and DTW have a better in-sample accuracy while soft-DTW has slightly better out-of-sample accuracy. We believe soft-DTW has better generalization capacity in future studies with more cases.

Table 1. Classifier performance based on different dissimilarity measure

Dissimilarity	In sample accuracy	LOO accuracy
Euclidean	0.79	0.52
DTW	0.84	0.58
Soft DTW	0.79	0.68

4. Discussion and Conclusion

In this study, we proposed a method to classify HCM subtypes via two-dimensional endocardial curvature. A pair of curvature series were aligned to each other to compute their dissimilarity/discrepancy. Dynamic time wrapping method and its variant soft-DTW were both used, which could eliminate the effect of varying series lengths and well capture the predominant characteristics in curvature series. The dissimilarity (DTW distance) was used to classify the curvature series into HCM subtypes. Classic K-nearest neighbors methods were used. DTW and soft-DTW obtain better classification accuracy than Euclidean

distance without alignment in our experiments.

Acknowledgements

This work was supported in part by grants from National Natural Science Foundation of China (NSFC 61562060,61801203),National Medical Research Council Grant (NMRC/EDG/1037/2013; NMRC/OFIRG/0018/2016), Natural Science Foundation of Jiangxi(20171BAB212008) Biomedical Research Council Research Grant (14/1/32/24/002).

References

[1] Kovacic J, Muller D. Hypertrophic cardiomyopathy: state-of-the-art review, with focus on the management of outflow obstruction. Internal medicine journal 2003;33(11):521–529.

[2] Hansen MW, Merchant N. Mri of hypertrophic cardiomyopathy: part i, mri appearances. American Journal of Roentgenology 2007;189(6):1335–1343.

[3] Wigle ED. The diagnosis of hypertrophic cardiomyopathy. Heart 2001;86(6):709–714.

[4] Elliott P, McKenna WJ. Hypertrophic cardiomyopathy. The Lancet 2004;363(9424):1881–1891.

[5] Hughes S. The pathology of hypertrophic cardiomyopathy. Histopathology 2004;44(5):412–427.

[6] Binder J, Ommen SR, Gersh BJ, Van Driest SL, Tajik AJ, Nishimura RA, Ackerman MJ. Echocardiography-guided genetic testing in hypertrophic cardiomyopathy: septal morphological features predict the presence of myofilament mutations. In Mayo Clinic Proceedings, volume 81. Elsevier, 2006; 459–467.

[7] Maron MS, Lesser JR, Maron BJ. Management implications of massive left ventricular hypertrophy in hypertrophic cardiomyopathy significantly underestimated by echocardiography but identified by cardiovascular magnetic resonance. The American journal of cardiology 2010; 105(12):1842–1843.

[8] Pattynama PM, De Roos A, Van der Wall EE, Van Voorthuisen AE. Evaluation of cardiac function with magnetic resonance imaging. American heart journal 1994;128(3):595–607.

[9] Ioannidis JP, Trikalinos TA, Danias PG. Electrocardiogram-gated single-photonemission computed tomography versus cardiacmagnetic resonance imaging for the assessmentof left ventricular volumes and ejection fraction: A meta-analysis. Journal of the American College of Cardiology 2002;39(12):2059–2068.

[10] Myerson SG, Bellenger NG, Pennell DJ. Assessment of left ventricular mass by cardiovascular magnetic resonance. Hypertension 2002;39(3):750–755.

[11] La Gerche A, Claessen G, Van de Bruaene A, Pattyn N, Van Cleemput J, Gewillig M, Bogaert J, Dymarkowski S, Claus P, Heidbuchel H. Cardiac mri a new gold standard for ventricular volume quantification during high-intensity exercise. Circulation Cardiovascular Imaging 2013;6(2):329–338.

[12] Rickers C, Wilke NM, Jerosch-Herold M, Casey SA, Panse P, Panse N, Weil J, Zenovich AG, Maron BJ. Utility of cardiac magnetic resonance imaging in the diagnosis of hypertrophic cardiomyopathy. Circulation 2005;112(6):855–861.

[13] Zhong L, Su Y, Yeo SY, Tan RS, Ghista DN, Kassab G. Left ventricular regional wall curvedness and wall stress in patients with ischemic dilated cardiomyopathy. American Journal of Physiology Heart and Circulatory Physiology 2009;296(3):H573–H584.

[14] Zhong L, Gobeawan L, Su Y, Tan JL, Ghista D, Chua T, Tan RS, Kassab G. Right ventricular regional wall curvedness and area strain in patients with repaired tetralogy of fallot. American Journal of Physiology Heart and Circulatory Physiology 2012;302(6):H1306–H1316.

[15] Noureldin RA, Liu S, Nacif MS, Judge DP, Halushka MK, Abraham TP, Ho C, Bluemke DA. The diagnosis of hypertrophic cardiomyopathy by cardiovascular magnetic resonance. Journal of Cardiovascular Magnetic Resonance 2012;14(1):17.

[16] Lee LC, Ge L, Zhang Z, Pease M, Nikolic SD, Mishra R, Ratcliffe MB, Guccione JM. Patient-specific finite element modeling of the cardiokinetix parachute® device: effects on left ventricular wall stress and function. Medical biological engineering computing 2014;52(6):557–566.

[17] Zhao X, Tan RS, Tang HC, Teo SK, Su Y, Wan M, Leng S, Zhang JM, Allen J, Kassab GS, et al. Left ventricular wall stress is sensitive marker of hypertrophic cardiomyopathy with preserved ejection fraction. Frontiers in physiology 2018;9:250.

[18] Teo SK, Zhao X, Tan RS, Zhong L, Su Y. Characterization of hypertrophic cardiomyopathy using left ventricular regional wall thickness derived from cmr imaging. In Computing in Cardiology (CinC), 2017. IEEE, 2017; 1–4.

[19] Sakoe H. Dynamic-programming approach to continuous speech recognition. In 1971 Proc. the International Congress of Acoustics, Budapest. 1971; .

[20] Sakoe H, Chiba S. Dynamic programming algorithm optimization for spoken word recognition. IEEE transactions on acoustics speech and signal processing 1978;26(1):43–49.

[21] Cuturi M, Vert JP, Birkenes O, Matsui T. A kernel for time series based on global alignments. In Acoustics, Speech and Signal Processing, 2007. ICASSP 2007. IEEE International Conference on, volume 2. IEEE, 2007; II–413.

[22] Cuturi M, Blondel M. Soft-dtw: a differentiable loss function for time-series. arXiv preprint arXiv170301541 2017; .

Address for correspondence:

Liang Zhong
National Heart Centre Singapore, 5 Hospital Drive, Singapore 169609
zhong.liang@nhcs.com.sg

Min Wan
Nanchang University, Nanchang, Jiangxi, P.R.China 330031
wanmin@ncu.edu.cn